

Synchronization of Networked Jahn-Teller Systems in Circuit QED

Yusuf Gül*

*Faculty of Engineering and Natural Sciences, Sabanci University, Orhanli-Tuzla, Istanbul, Turkey and
Department of Physics, Boğaziçi University 34342 Bebek, Istanbul, Turkey*

(Dated: November 4, 2016)

We consider the nonlinear effects in Jahn-Teller system of two coupled resonators interacting simultaneously with flux qubit using Circuit QED. Two frequency description of Jahn Teller system that inherits the networked structure of both nonlinear Josephson Junctions and harmonic oscillators is employed to describe the synchronous structures in multifrequency scheme. Emergence of dominating mode is investigated to analyze frequency locking by eigenvalue spectrum. Rabi Supersplitting is tuned for coupled and uncoupled synchronous configurations in terms of frequency entrainment switched by coupling strength between resonators. Second order coherence functions are employed to investigate self-sustained oscillations in resonator mode and qubit dephasing. Synchronous structure between correlations of privileged mode and qubit is obtained in localization-delocalization and photon blockade regime controlled by the population imbalance.

PACS numbers: 42.50.Pq, 71.70.Ej, 85.25.-j

I. INTRODUCTION

Advances in control and flexibility of quantum mechanical systems leads to the era of quantum simulators such as ultracold atoms[1, 2], ion traps [3, 4] and cavity QED arrays[5, 6] in the line with the general program of simulating a physical system with another. Exploring fundamental quantum mechanics in lattice arrays of Circuit QED [7, 8] and embedding the artificial atoms into open transmission line resonators [9, 10] bring another suitability criteria in strong and ultrastrong coupling regimes for quantum information processing [11–14]. Emergence of cooperativity and synchronization in collective behavior of many body coupled systems trigger quantum classical transitions in small scales [15–18] and tunable correlations for large scale systems [19–22].

In solid state systems, Cooperative Jahn-Teller (CJT) systems give rise to structural phase transitions including both linear and quadratic interaction in definite crystal geometries[23, 24]. Previously, $E \otimes (b_1 + b_2)$ model is investigated for nonlinear effects by variational principles in [26]. Nonlinearities lead to the asymmetry of the interaction strengths and the chaotic patterns in energy levels of two coupled oscillators [27]. Lattice array of localized JT centers are examined as an extension of Dicke model [28].

Superconducting Quantum Interference Devices (SQUIDS) appear as an electrical analog platform to simulate the collective behavior of particles trapped in local minima of double well potentials warped by the nonlinearities [29]. Circuit QED architectures inherits the nonlinear characteristics of Josephson Junctions leading to the emergence of spatial and temporal transitions in coupled resonator schemes. Two regimes of coherent oscillations and self trapping by controlled non-

linearities are analyzed in a hybrid system [30] composed of bosonic Josephson Junction [31, 32]. Localization delocalization transitions are shown in photon JJ in Circuit QED setup [33] embedded in a Jaynes-Cummings (JC) lattice array [34, 35].

In Josephson Junction Arrays (JJAs), due to the collective behavior of Cooper pairs, synchronization desynchronization transitions comes out in phase coherence pattern[36–38]. In spatially extended systems, cluster of oscillator networks have the ability of tuning transitions locally as a result of coupling strengths relaxing towards the localized dominating node[39]. Optomechanical systems, as lumped model of two coupled harmonic oscillator via light, appear as test bed for reduced form of the effective Kuramoto model in dissipative environment and reconfigurable synchronous oscillator networks [40, 41].

Our aim is to employ Cavity/Circuit QED realization of JT models [42, 43] to exhibit the effect of nonlinearities in multifrequency coupled resonator schemes. Coupled modes of resonators over which the JT coupling distribution can be tuned to manipulate synchronization of qubit dephasing and population imbalance in terms of normal modes conveying Josephson Junction nonlinearities [44, 45]. Quadratic interactions, responsible for warping in JT systems networked to the outer circuitry, appear as the nonlinear Josephson inductance coupling between the flux qubit and the plasma mode [46–48]. We present the effect of quadratic interaction in synchronization of two frequency JT systems. Our system is composed of two coupled resonators interacting simultaneously with a single flux qubit resembling the minimal coupled models of strongly correlated spin-boson systems on a lattice [49, 50].

This paper is organized as follows. In Sec.II we introduce the coupled model with quadratic interactions and use effective single mode transformation. The results and discussions are presented in Sec.III. Finally, we give conclusions in Sec. VI.

*Electronic address: yusufgul.josephrose@gmail.com.

II. MODEL

Circuit QED simulations of JT-models requires both multi-frequency description of vibrational interactions and going beyond the Rotating Wave Approximation (RWA) due to the ultrastrong coupling regime. Our model hamiltonian is ($\hbar = 1$)

$$H = \frac{\omega}{2}\sigma_z + \sum_{i=1,2} \omega_i a_i^\dagger a_i + \lambda_i (a_i + a_i^\dagger) \sigma_x + \sum_{i=1,2} g_i (a_i + a_i^\dagger)^2 \sigma_x \quad (1)$$

$$H_{NL} = [\omega_{eff}(\alpha_1 + \alpha_1^\dagger)^2 + \omega'(\alpha_2 + \alpha_2^\dagger)^2 + J(\alpha_1 + \alpha_1^\dagger)(\alpha_2 + \alpha_2^\dagger)]\sigma_x \quad (2)$$

where ω and $\omega_{1,2}$ are the qubit and resonator frequencies. $a_{1,2}(a_{1,2}^\dagger)$ represents the annihilation and creation operators of resonators and σ_x, σ_z are the Pauli operators. This hamiltonian shows the coupling between flux qubit and two plasma mode in both linear and nonlinear interaction strengths $\lambda_{1,2}$ and $g_{1,2}$ respectively. To go beyond RWA, Circuit QED realization of our system is mapped to two frequency JT model and described as

$$H = H_q + H_r + H_{JT} + H_{NL}, \quad (3)$$

where

$$H_q = \frac{\omega}{2}\sigma_z \quad (4)$$

$$H_r = \omega_1 a_1^\dagger a_1 + \omega_2 a_2^\dagger a_2 \quad (5)$$

are the qubit and resonator hamiltonians with natural frequencies in uncoupled scheme. The Jahn-Teller interaction is given by

$$H_{JT} = k_1 \omega_1 (a_1 + a_1^\dagger) \sigma_x + k_2 \omega_2 (a_2 + a_2^\dagger) \sigma_x \quad (6)$$

where $k_{1,2}$ are the dimensionless JT scaling factors [43, 51, 52]. In the absence of Nonlinear term, our system behaves as an effective single mode model where the qubit coupled to resonators asymmetrically due to the concentration of JT interaction in privileged mode.

Quadratic interaction terms appear due to the nonlinear Josephson inductance in SQUID phase leading to the occurrence of second order terms corresponding to the fluctuations of dynamical variables controlled by the external parameters [46–48]. In JT systems, quadratic interactions are determined empirically and depend on the symmetry lowering configurations of crystal geometries. Then, hamiltonian describing quadratic interactions is written as

$$H_{NL} = [\omega_1 (a_1 + a_1^\dagger)^2 + \omega_2 (a_2 + a_2^\dagger)^2] \sigma_x \quad (7)$$

which makes the system networked to outer crystal structure described as bath of harmonic oscillators with natural frequencies $\omega_{1,2} = g_{1,2}$ in spin-boson treatment. Using both linear and nonlinear coupling, our system in two frequency effective JT model [43, 51, 52] becomes

$$H = H_{JT} + H_{NL} \quad (8)$$

where

$$H_{JT} = \frac{\omega}{2}\sigma_z + \omega' \alpha_2^\dagger \alpha_2 + J(\alpha_1^\dagger \alpha_2 + \alpha_2^\dagger \alpha_1) + \omega_{eff}[\alpha_1^\dagger \alpha_1 + k_{eff}(\alpha_1 + \alpha_1^\dagger)\sigma_z] + c_2[(\alpha_1^\dagger \alpha_2 + \alpha_1 \alpha_2^\dagger) + k_{eff}(\alpha_2^\dagger + \alpha_2)\sigma_z] \quad (9)$$

and

$$H_{NL} = [\omega_{eff}(\alpha_1 + \alpha_1^\dagger)^2 + \omega'(\alpha_2 + \alpha_2^\dagger)^2 + J(\alpha_1 + \alpha_1^\dagger)(\alpha_2 + \alpha_2^\dagger)]\sigma_x \quad (10)$$

with the frequency of effective mode

$$\omega_{eff} = \frac{\omega_1 k_1^2 + \omega_2 k_2^2}{k_{eff}} \quad (11)$$

and qubit-resonator coupling strength

$$k_{eff}^2 = k_1^2 + k_2^2. \quad (12)$$

The frequency of the disadvantaged mode is given by

$$\omega' = \frac{\omega_1 k_2^2 + \omega_2 k_1^2}{k_{eff}} \quad (13)$$

and it is coupled to the privileged mode with a strength

$$c_2 = \frac{\Delta k_1 k_2}{k_{eff}^2}. \quad (14)$$

where the frequency mismatch $\Delta = \omega_1 - \omega_2$ is used to control the perturbative interactions on the effective single-mode model.

For simulation purposes, we use two parameters (k, Δ) to see the effect of JT scaling factors and frequency difference of the resonators in going beyond RWA. For this purpose our Circuit QED Hamiltonian is written as

$$H = \hat{\alpha}_1^\dagger \hat{\alpha}_1 + \hat{\alpha}_2^\dagger \hat{\alpha}_2 + \frac{1}{2}\sigma_z + \frac{\Delta}{2}(\hat{\alpha}_1^\dagger \hat{\alpha}_2 + \hat{\alpha}_2^\dagger \hat{\alpha}_1) + \sqrt{2}k[(\hat{\alpha}_1^\dagger + \hat{\alpha}_1) + (\hat{\alpha}_1^\dagger + \hat{\alpha}_1)^2 + \frac{\Delta}{2}((\hat{\alpha}_2^\dagger + \hat{\alpha}_2) + (\hat{\alpha}_2^\dagger + \hat{\alpha}_2)^2)]\sigma_x. \quad (15)$$

where $k_1 = k_2 = k$, $\lambda_1 = (\omega_1 + \omega_2)k/\sqrt{2}$, $\lambda_2 = \Delta k/\sqrt{2}$, and $c_2 = \Delta/2$. We present the coupling of two resonator with the hopping parameter $J = c_2$.

In this manner, we consider our coupled system as coupling of privileged mode interacting simultaneously with the qubit and the disadvantaged mode. Correlations of privileged mode and population imbalance between resonators give rise to cooperative and synchronous JT systems in Circuit QED.

III. RESULTS

Externally controlled nonlinearities wired with the JT models make the coupled systems plausible for emergence of cooperativity and synchronization in singled out mode in both strong and ultrastrong regime.

In JJAs, distribution of frequencies are modulated so as to make the nonlinear oscillators frequency locked corresponding to the Kuramoto model of mean field theories [37]. In two frequency JT model, appearance of singled out effective mode is investigated in terms of scaling factors k dominating privileged mode and frequency difference Δ representing the coupling strength of perturbations.

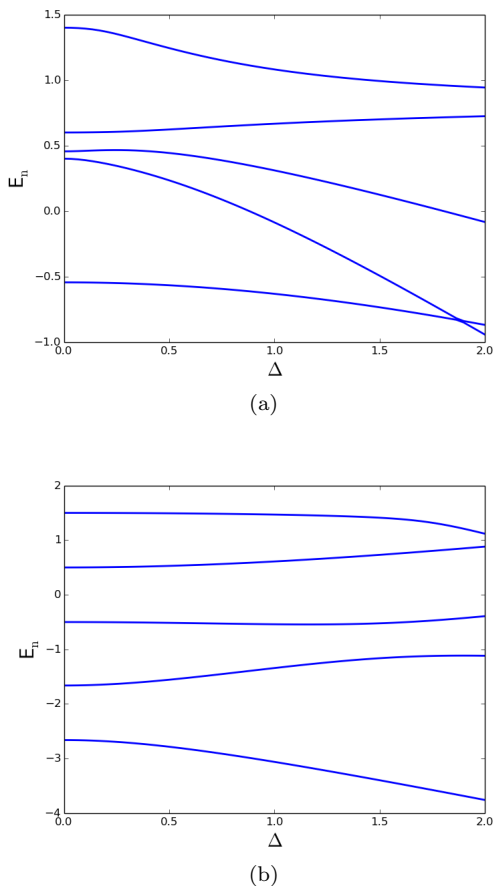


FIG. 1: (Color online) Emergence of frequency locking for two-mode JT system shown in spectrum of the lowest five eigenvalues depending on the frequency difference Δ . (a) At $\Delta = 0$ Rabi splitting of first energy levels occurs for $k = 0.1/\sqrt{2}$. Interaction between privileged and disadvantaged mode can be tuned up to $\Delta = 0.1$ in single effective mode. (b) Range of single mode regime extends up to $\Delta = 0.5$ in ultrastrong regime $k = 1.0/\sqrt{2}$

We examined 5 lowest eigenenergies in the spectrum of our system where each resonator is described with Fock space dimension 2. In Fig.2., we present the tendency of

frequency locking structure of our system in both strong and ultrastrong regimes. Our system is in single privileged mode only for frequency difference $|\Delta| < 0.1$ and $k = 0.1/\sqrt{2}$ plotted in fig.2(a). Effect of perturbative coupling leads to pure Rabi splitting of first excited level for $|\Delta| = 0$. In Fig.2(b), when we are in ultrastrong regime for $k = 1.0/\sqrt{2}$ the range of single mode structure extends up to $|\Delta| < 0.5$ and avoiding crossing is replaced with a level repelling. The pattern of eigenvalue spectrum is mixed by $|\Delta|$ and smoothed by k exhibiting the competition between linear and nonlinear interaction terms.

Circuit QED realizations of vacuum Rabi splitting is detected by the transmitted amplitude of field quadratures in an array of transmon qubits coupled with a common resonator [13]. Linear JT model of two mode coupled systems shows frequency conversion modulated by nonlinear susceptibility [14]. Circuit QED setup is chosen so as to make it appropriate for transmission measurement and macroscopic quantum coherence in quantum classical transition [53, 56].

We use the two time correlation spectrum of heterodyne transmission spectrum for the privileged mode $\hat{\alpha}_1$, so that

$$P(\omega) = \int_{-\infty}^{\infty} \langle \hat{\alpha}_1(t) \hat{\alpha}_1(0) \rangle e^{-i\omega t} dt. \quad (16)$$

Open system dynamics is governed by

$$\frac{d\rho}{dt} = -i[H, \rho] + \mathcal{L}\rho, \quad (17)$$

where the Liouvillian superoperator \mathcal{L} is given by

$$\begin{aligned} \mathcal{L}\rho = & \sum_{j=1,2} (1 + n_{th}) \kappa \mathcal{D}[\hat{\alpha}_j] \rho + n_{th} \kappa \mathcal{D}[\hat{\alpha}_j^\dagger] \rho \\ & + \gamma \mathcal{D}[\sigma] \rho + \frac{\gamma_\phi}{2} \mathcal{D}[\sigma_z] \rho, \end{aligned} \quad (18)$$

with n_{th} representing the average thermal photon number. Taking $n_{th} = 0.15$ corresponds to 100 mK [43, 56]. \mathcal{D} denotes the Lindblad type damping superoperators, κ is the cavity photon loss rate. Qubit relaxation and dephasing rates are, respectively, γ and γ_ϕ . We use balanced dissipation where resonator decay parameters $\kappa_1 = \kappa_2 = 0.001$ and qubit relaxation and dephasing parameters $\gamma = 0.001, \gamma_\phi = 0.01$ with the thermal occupation number $n_{th} = 0.15$.

Fig.2 shows nonlinear vacuum response of the cavity field for hopping parameter $J = 0$ and $J = 0.5$ values. Fig.2(a) presents asymmetric Rabi peaks in Lorentzian line shape when the system is in single mode JC regime. Increasing the coupling strength reveals the emergence of supersplitting of each vacuum Rabi peak into a doublet with a higher amplitude. Fig.2(b) shows the Rabi supersplitting for $k = 0.05$. Going beyond the single mode JC regime increase the central dip in each peaks. Effect of hopping parameters is seen in multi-photon transitions.

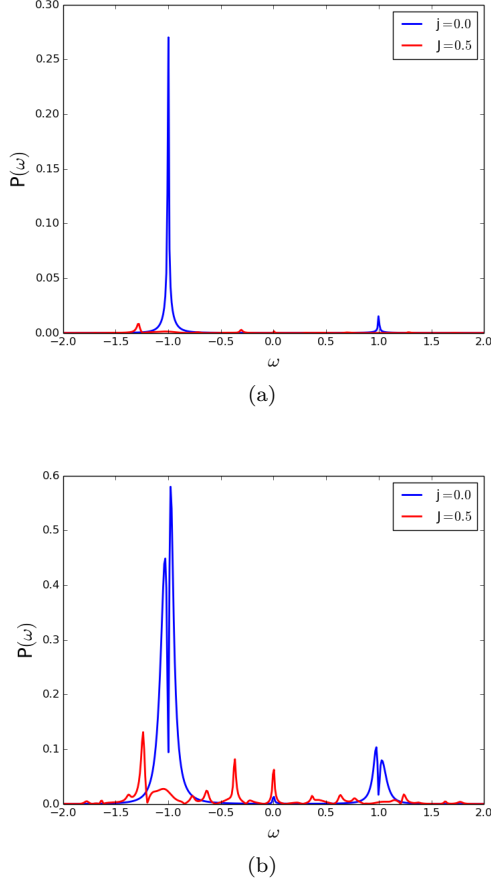


FIG. 2: (Color online) Correlation spectrum of privileged mode α_1 in coupled, and uncoupled scheme depending on hopping parameter J . (a) Asymmetric peaks of Lorentzian line shape in uncoupled, $J = 0$ and coupled, $J = 0.5$, resonators in single mode regime $k = 0.05\sqrt{2}$ (b) Rabi supersplitting occurs for $k = 0.05$ together with the multilevel transitions.

when the number of subpopulations in variants of Kuramoto model is equal to the degrees of freedom of the system under considerations, one can obtain reconfigurations of coupled and uncoupled schemes by tuning frequency mismatch with (k, Δ) parameters. In coupled resonator scheme, $\Delta \neq 0$, hopping terms appears as the inter-cavity control parameter resulting in cooperative and synchronous structure. Field quadratures are used in describing measure of quantum analogue of frequency entrainment and locking in optomechanical systems and harmonically driven Van der Pol oscillator[57, 58]. Self-sustained oscillation is shown in amplitude locking with quadratic coupling leading to multipeak field spectrum [59].

Fig. 3 presents how the coupling regime dominates the inherited features of nonlinear Josephson Junctions depending on the configurations. Fig. 3(a) shows the shift of splitted peaks from each other and raise of extra peak around $\omega = 0$ for $k = 0.1$ which indicates the syn-

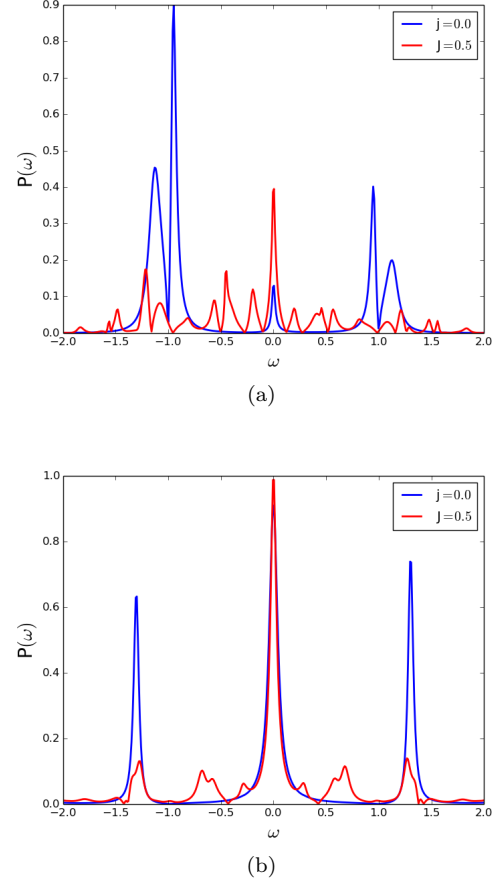


FIG. 3: (Color online) Appearance of stokes anti-stokes peaks in two mode JC regime. (a) Shift of side peaks in strong coupling regime $k = 0.1/\sqrt{2}$ and nonlinear response of the system is shown by the increase central dip of each side peak (b) At intermediate coupling regime $k = 0.5/\sqrt{2}$. asymmetry occurs in side peaks and amplitude of the central peak gets higher than the others. Coincidence of the central and side peaks is used for the synchronous schemes for coupled and uncoupled configurations.

chronization entrainment although their amplitude is still different. In Fig. 3(b), at intermediate coupling regime $k = 0.5$, spectrum evolve into a triplet where the asymmetry of peaks are tuned in terms of relative coupling between privileged and disadvantaged mode. Emergence of stokes and anti-stokes peaks are due to field quadrature operator which behaves as qubit-polariton operator revealing Raman process. Coherent evolution is modulated by the multilevel structure of atomic states carrying the nonlinearities of JJs intrinsically. The frequency amplitude of coupled and uncoupled scheme gets closer and is coincident in both central and side peaks in definite frequencies. Switchable synchronous configurations are obtained by synchronization entrainment between the pure two mode JT and the effective privileged mode model.

Two frequency realization of Circuit QED architec-

tures appears as a platform to simulate the self-sustained oscillator behavior of tetrahedral networks distorted by corner sharing spin, where nonlinearities are induced by the lattice restoring energy. Switching symmetric and asymmetric mode configurations leads to the transverse and longitudinal prolongation of host lattice arrangement mimicking the rhythmic behavior of diamond shaped crystal geometries. Accumulate and fire oscillators description give way to slow growth of correlations similar to the van der Pol relaxation oscillator [22, 57, 58] in the presence of distortions. In our model, self-sustained oscillation of each normal mode is described by correlations revealing delocalization and trapping regimes of coupled system.

In order to see the correlations of distortions, we use the second order coherence functions of field and atomic states

$$g_i^{(2)} = \frac{O_i^\dagger(t)O_i^\dagger(t+\tau)O_i(t)O_i(t+\tau)}{O_i^\dagger(t)O_i(t)} \quad (19)$$

where $i = r, q$ are used in place of the resonator and the qubit respectively.

The condition $g_{r,q}^{(2)} \ll 1$ corresponds to antibunching, and used for the indication of photon blockade and energetic localization of qubit. Another central quantity of coupled cavity system is the photon population imbalance $z(t) = (n_1 - n_2)/(n_1 + n_2)$ where $n_i = \text{Tr} \hat{\alpha}_i^\dagger \hat{\alpha}_i \hat{\rho}$ for $i = 1, 2$ corresponds to the two cavities described by privileged and disadvantaged mode. Total photon number is given by $N = n_1 + n_2$. In performing calculations we take $N = 5$ and both of the privileged mode and qubit are excited initially.

In Fig.4 we show the correlations functions of resonator and qubit in weak, strong and ultrastrong regimes. In the first two top panels, we present the second order coherence functions of privileged mode (blue) and the qubit (red) and the third panel shows population imbalance (green). Fig.4.a shows correlations and population imbalance in weak coupling regime, $k = 0.01/\sqrt{2}$. Population imbalance is in oscillating regime and synchronous with the photon correlation. Self-sustained oscillation is seen via decreasing of population imbalance while resetting of antibunching of privileged mode at two different time scales corresponding to accumulate and fire oscillator in the sense of van der Pol relaxation. As τ increases population imbalance reaches zero and qubit correlation with beats in anharmonic time intervals become stable. Starting with $g_{r,q}^{(2)}(0) = 0$ corresponding to the photon blockade regime, photon correlations reach stable point with decreasing peaks while onsite repulsion is increasing. In strong regime $k = 0.1/\sqrt{2}$, fig.4.b shows the delocalization-localization transitions in population imbalance. Contrary to the weak coupling regime, qubit and photon correlation becomes synchronous representing simultaneous firing and damping of correlations as τ increases. Although accumulation gets diminished in blockade regime, there is still firing of qubit and privileged mode correlation due to the multilevel transitions

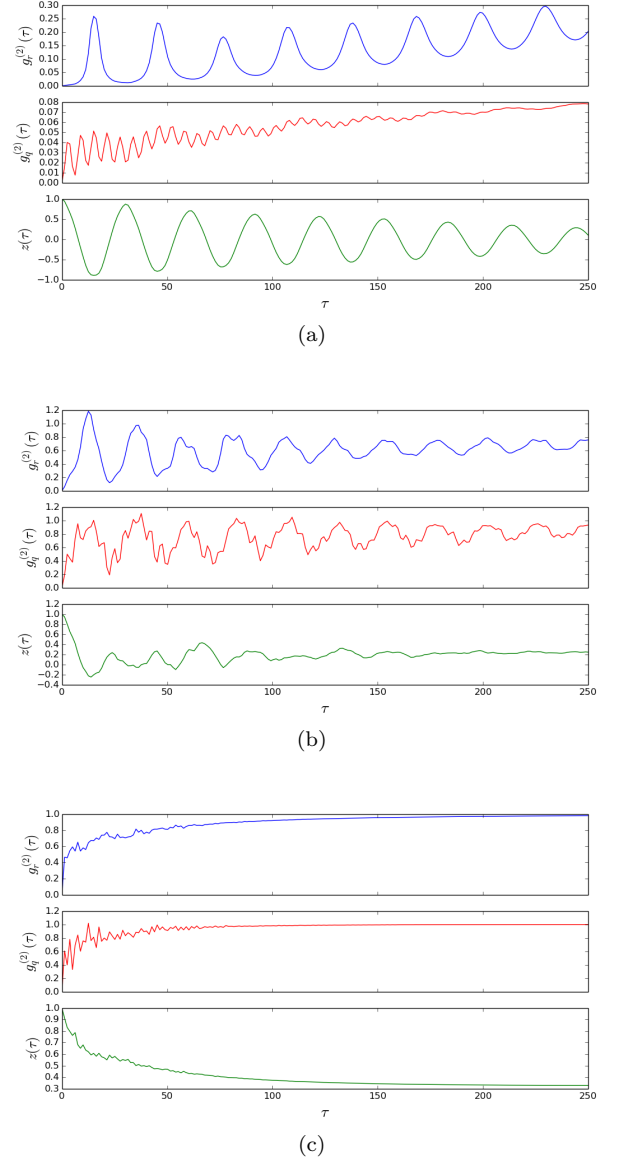


FIG. 4: (Color online) Emergence of localization and synchronization transitions in weak, strong and ultrastrong regime. (a) shows synchronous structure between damped oscillating population imbalance and correlation of privileged mode in weak coupling $k = 0.01/\sqrt{2}$. (b) privileged mode becomes synchronous with qubit and delocalization-localization transition occurs in population imbalance in strong coupling regime $k = 0.1/\sqrt{2}$. (c) presents the photon blockade in privileged mode and fully trapped regime in population imbalance with $k = 1.0/\sqrt{2}$ and $\gamma_\phi = 0.1$

by the inherited nonlinearities of JJs. Fig.4.c presents the fully localized regime for population imbalance and all the quantities reach a stable point in ultra-strong regime, $k = 1.0/\sqrt{2}$. Effect of qubit dephasing is shown by quenching thermal fluctuations by taking $\gamma_\phi = 0.1$ and leaving the other parameters the same.

These results suggest that two frequency description JT system can be used to investigate cooperative and synchronous behaviors of circuit QED schemes by modulating the qubit anharmonicities due to JJs with networked nonlinearities.

IV. CONCLUSION

In conclusion, we have shown that nonlinearities play a central role in describing the cooperativity and synchronization in Circuit QED architectures by the inherited nonlinearities of Josephson Junctions. In our model, flux qubit simultaneously is coupled to two resonator with both linear and quadratic interaction terms. We performed the eigenenergy and power spectrum calculations

in frequency locking and synchronization entrainment regimes respectively. Nonlinearities give way to exploration of quantum mechanics at the fundamental level such as Rabi Super-splitting. Tetrahedral structures of JT systems opens the way of constructing networked oscillators which can be translated to coupled resonator schemes of circuit QED. Correlation functions of normal modes and qubit indicate cooperative and synchronous structures in localization delocalization and photon blockade regimes.

Acknowledgments

Y. G. gratefully acknowledges support by Boğaziçi University BAP project no 6942.

-
- [1] M. Lewenstein *et al.*, *Traveling to exotic places with ultracold atoms*, Aip Conference Proceedings Vol. 869 (Am. Inst. Physics, Melville, 2006), pp. 201–211.
 - [2] I. Bloch, J. Dalibard, and W. Zwerger, *Rev. Mod. Phys.* **80**, 885 (2008).
 - [3] D. Porras, J. I. Cirac, *Phys. Rev. Lett.* **92**, 207901 (2004).
 - [4] D. Porras, P. A. Ivanov, and F. Schmidt-Kaler *Phys. Rev. Lett.* **108**, 235701 (2012).
 - [5] M. Hartmann, F. Brandão, and M. Plenio, *Laser Photon. Rev.* **2**, 527 (2008).
 - [6] A. D. Greentree, C. Tahan, J. H. Cole, and L. Hollenberg, *Nature Phys.* **2**, 856 (2006).
 - [7] A. A. Houck, H. E. Türeci, and J. Koch, *Nature Phys.* **8**, 292 (2012).
 - [8] S. Schmidt and J. Koch, *Ann. Phys.* **525**, 395 (2013).
 - [9] B. Peropadre, D. Zueco, D. Porras, J. J. García-Ripoll, *Phys. Rev. Lett.* **111**, 243602 (2013).
 - [10] A. A. Abdumalikov, O. Astafiev, A. M. Zagoskin, Yu. A. Pashkin, Y. Nakamura, and J. S. Tsai *Phys. Rev. Lett.* **104**, 193601 (2010).
 - [11] A. Blais, Ren-Shou Huang, A. Wallraff, S. M. Girvin, and R. J. Schoelkopf *Phys. Rev. A* **69**, 062320 (2004).
 - [12] J. Bourassa, J. M. Gambetta, A. A. Abdumalikov, Jr., O. Astafiev, Y. Nakamura, and A. Blais *Phys. Rev. A* **80**, 032109 (2009).
 - [13] L. S. Bishop, J. M. Chow, Jens Koch, A. A. Houck, M. H. Devoret, E. Thuneberg, S. M. Girvin and R. J. Schoelkopf *Nature Physics* **5**, 105 (2009).
 - [14] K. Moon and S. M. Girvin *Phys. Rev. Lett.* **95**, 140504 (2005).
 - [15] A. Smerzi, S. Fantoni, S. Giovanazzi, S. R. Shenoy, *Phys. Rev. Lett.* **79**, 4950 (1997).
 - [16] S. Raghavan, A. Smerzi, S. Fantoni, S. R. Shenoy, *Phys. Rev. A* **59**, 620 (1999).
 - [17] M. Abbarchi, A. Amo, V. G. Sala, D. D. Solnyshkov, H. Flayac, L. Ferrier, I. Sagnes, E. Galopin, A. Lematre, G. Malpuech and J. Bloch *Nature Phys.* **9**, 275 (2013).
 - [18] J. Raftery, D. Sadri, S. Schmidt, H. E. Türeci, and A. A. Houck *Phys. Rev. X* **4**, 031043 (2014).
 - [19] H. Qiu, Bruno Juliá-Díaz, M. Angel Garcia-March, and A. Polls *Phys. Rev. A* **90**, 033603 (2014).
 - [20] I. Hermoso de Mendoza, *et al.* *Phys. Rev. E* **90**, 052904 (2014).
 - [21] A. Arenas, *et al.* *Phys. Rep.* **469**, 93 (2014).
 - [22] A. S. Pikovsky, M. Rosenblum, and J. Kurths, *Synchronization: A Universal Concept in Nonlinear Science* (Cambridge University Press, New York, 2001).
 - [23] M. J. D. Kaplan and B. G. Vekhter, *Cooperative Phenomena in Jahn Teller Phenomena* (Plenum, New York, 1995).
 - [24] Z. Popovic and S. Satpathy, *Phys. Rev. Lett.* **84**, 1603 (2000).
 - [25] Y. Yamashita and K. Ueda *Phys. Rev. Lett.* **85**, 4960 (2000).
 - [26] E. Majerníková and S. Shpyrko *J. Phys.: Condens. Matter* **15** 2137 (2003).
 - [27] E. Majerníková and S. Shpyrko *Phys. Rev. E* **73**, 057202 (2006).
 - [28] E. Majerníková and S. Shpyrko *J. Phys. A: Math. Theor.* **44** 06510 (2011).
 - [29] V. Lefevre-Seguin *et al.*, *Phys. Rev. B* **46**, 5507 (1992).
 - [30] R. J. Schoelkopf and S. M. Girvin *Nature* **451**, 664 (2008).
 - [31] M. Albiez, R. Gati, J. Fölling, S. Hunsmann, M. Cristiani, and Markus K. Oberthaler *Phys. Rev. Lett* **95**, 010402 (2005).
 - [32] N. Didier, S. Pagnetti, Y. M. Blanter, and Rosario Fazio *Phys. Rev. B* **84**, 054503 (2011).
 - [33] S. Schmidt, D. Gerace, A. A. Houck, G. Blatter, and H. E. Türeci *Phys. Rev. B* **82**, 100507 (2010).
 - [34] F. Nissen, S. Schmidt, M. Biondi, G. Blatter, H. E. Türeci, and J. Keeling *Phys. Rev. Lett.* **108**, 233603 (2012).
 - [35] T. Hümmer, G. Reuther, P. Hänggi, D. Zueco, *Phys. Rev. A* **85**, 052320 (2012).
 - [36] K. Wiesenfeld, P. Colet, S. H. Strogatz, *Phys. Rev. Lett.* **76**, 404 (1996).
 - [37] K. Wiesenfeld, P. Colet, S. H. Strogatz, *Phys. Rev. E* **57**, 1563 (1998).
 - [38] Shi-Zeng Lin, Xiao Hu, and Lev Bulaevskii, *Phys. Rev. B* **84**, 104501 (2011).
 - [39] G. Manzano, F. Galve, G. L. Giorgi, E. Hernández-García, and R. Zambrini, *Sci. Rep.* **3**, 1439 (2013).
 - [40] G. Heinrich, M. Ludwig, J. Qian, B. Kubala and F. Mar-

- quardt Phys. Rev. Lett. **107**, 043603(2011).
- [41] M. Zhang, G. S. Wiederhecker, S. Manipatruni, A. Barnard, P. McEuen and Michal Lipson Phys. Rev. Lett. **109**, 233906(2012).
 - [42] J. Larson, Physical Review A **78**, 033833 (2008).
 - [43] T Dereli, Y. Gül, P. Forn-Díaz, Ö. E. Müstecaplıoğlu, Phys. Rev. A. **85**, 053841 (2012).
 - [44] F. Lecocq, J. Claudon, O. Buisson, and P. Milman Phys. Rev. Lett. **107**, 197002 (2011).
 - [45] F. Lecocq, I. M. Pop, I. Matei, E. Dumur, A.K. Feofanov, C. Naud, W. Guichard, and O. Buisson Phys. Rev. Lett. **108**, 107001(2012).
 - [46] P. Bertet, I. Chiorescu, G. Burkard, K. Semba, C. J. P. M. Harmans, D. P. DiVincenzo, and J. E. Mooij Phys. Rev. Lett. **95**, 257002 (2005).
 - [47] Georg M. Reuther, David Zueco, P. Hänggi, Sigmund Kohler, New J. Phys. **13**, 93022 (2011).
 - [48] P. Bertet, I. Chiorescu, C. J. P. M. Harmans, and J. E. Mooij arXiv (2005)cond-mat/0507290v1.
 - [49] Peter A. Ivanov, J. Low Temp. Physics **179**, 375, (2015).
 - [50] A. Kurcz, A. Bermudez, J. J. García-Ripoll Phys. Rev. Lett. **112**, 180405(2014).
 - [51] M. O'Brien J.Phys.C **5**, 2045 (1972).
 - [52] M. O'Brien J.Phys.C **16**, 85 (1983).
 - [53] A. Fedorov, P. Macha, A. K. Feofanov, C. J. P. M. Harmans, J. E. Mooij Phys. Rev. Lett. **106**, 170404(2011).
 - [54] Yu-xi Liu, J. Q. You, L. F. Wei, C. P. Sun and Franco Nori Phys. Rev. Lett. **95**, 087001(2005).
 - [55] J.Q. You and Franco Nori, Nature **474**, 589 (2011).
 - [56] J. M. Fink, L. Steffen, P. Studer, L. S. Bishop, M. Baur, R. Bianchetti, D. Bozyigit, C. Lang, S. Filipp, P. J. Leek, and A. Wallraff, Phys. Rev. Lett. **105**, 163601(2010).
 - [57] A. Mari, A. Farace, N. Didier, V. Giovannetti, and R. Fazio Phys. Rev. Lett. **111**, 103605(2013).
 - [58] S. Walter, A. Nunnenkamp, and C. Bruder Phys. Rev. Lett. **112**, 094102(2014).
 - [59] Lin Zhang and Hong-Yan Kong Physical Review A **89**, 023847 (2014).